

Supporting Information

for

Electrostatic repulsion causes anticooperative DNA binding between tumor suppressor  
ETS transcription factors and JUN-FOS at composite DNA sites

**Bethany J. Madison<sup>1,2§</sup>, Kathleen A. Clark<sup>1,2§</sup>, Niraja Bhachech<sup>1,2</sup>,  
Peter C. Hollenhorst<sup>3</sup>, Barbara J. Graves<sup>1,2,4\*</sup>, Simon L. Currie<sup>1,2#</sup>**

From the <sup>1</sup>Department of Oncological Sciences and <sup>2</sup>Huntsman Cancer Institute, University of  
Utah School of Medicine, Salt Lake City UT, 84112; <sup>3</sup>Medical Sciences, Indiana University  
School of Medicine, Bloomington IN, 47405; <sup>4</sup>Howard Hughes Medical Institute, Chevy Chase  
MD, 20815

<sup>§</sup>Both authors contributed equally to this work.

<sup>#</sup>Present address: Department of Biophysics, University of Texas Southwestern Medical Center,  
Dallas, Texas 75390

\*To whom correspondence should be addressed: Barbara J. Graves: Tel.: 1-301-215-8718; Fax:  
1-201-215-8828; Email: [Barbara.graves@hci.utah.edu](mailto:Barbara.graves@hci.utah.edu).

## Supporting Information

- S-3 Table S1. Equilibrium dissociation constants ( $K_D$ ) for ETS proteins binding to *UPP* promoter DNA with and without JUN-FOS.
- S-4 Table S2. Equilibrium dissociation constants ( $K_D$ ) for EHF and ERG binding to different DNA sequences.
- S-5 Table S3. Peak coordinates for ERG-FLAG and EHF-FLAG occupied regions in RWPE1 cells.
- S-6 Table S4. RSAT analysis of ETS-AP1 spacing in top 1000 peaks of ERG and EHF CHIP datasets.
- S-7 Table S5. Equilibrium dissociation constants ( $K_D$ ) for EHF truncations binding to *COPS8* enhancer DNA with and without JUN-FOS.
- S-8 Table S6. Equilibrium dissociation constants ( $K_D$ ) for EHF<sup>ΔN193</sup> mutants binding to *COPS8* DNA with and without JUN-FOS.
- S-9 Table S7. Equilibrium dissociation constants ( $K_D$ ) for ETS truncations binding to *COPS8* enhancer DNA with and without JUN-FOS.
- S-10 Table S8. Protein and DNA sequences used in this study.
- S-13 Table S9. qPCR primers used in this study.
- S-14 Figure S1. JUN-FOS differentially influences the DNA binding of ETS factors.
- S-15 Figure S2. ETS and AP1 sites are overrepresented at ERG- and EHF-bound genomic regions.
- S-16 Figure S3. The minimal DNA-binding domains of JUN and FOS are sufficient for anticooperative DNA binding with EHF.
- S-17 Figure S4. EHF and ERG have distinct JUN-FOS interfaces.
- S-18 Figure S5. Alignment of ETS domain and flanking sequences for human ETS factors.
- S-19 Figure S6. Positive residues on the JUN-FOS interface of EHF mediate anticooperative DNA binding.
- S-20 Figure S7. Diversification of charge in ETS factor evolution.
- S-21 Figure S8. The *ELF1* gene is frequently deleted in prostate cancer patients.
- S-22 Figure S9. Positively charged interface antagonizes simultaneous DNA binding with JUN-FOS in tumor suppressor ETS factors.

**Table S1. Equilibrium dissociation constants ( $K_D$ ) for ETS proteins binding to *UPP* promoter DNA with and without JUN-FOS.**

ETS <sup>1</sup>	DNA <sup>1</sup>	JUN-FOS <sup>1</sup>	$K_D$ (nM) <sup>2</sup>	n
EHF	<i>UPP</i>	+	2,000 ± 1,000	2
EHF	<i>UPP</i>	-	56 ± 7	2
SPDEF	<i>UPP</i>	+	2,000 ± 800	2
SPDEF	<i>UPP</i>	-	119 ± 9	2
ETV1	<i>UPP</i>	+	700 ± 400	2
ETV1	<i>UPP</i>	-	400 ± 200	2
ETV4	<i>UPP</i>	+	700 ± 300	2
ETV4	<i>UPP</i>	-	340 ± 30	2
ERG	<i>UPP</i>	+	65 ± 2	2
ERG	<i>UPP</i>	-	310 ± 30	2
FLI1	<i>UPP</i>	+	20 ± 10	2
FLI1	<i>UPP</i>	-	500 ± 300	2

<sup>1</sup> Full-length ETS and JUN-FOS proteins were used in this experiment; see Table S8 for protein and DNA sequences.

<sup>2</sup>  $K_D$  values are listed as mean ± standard deviation.

**Table S2. Equilibrium dissociation constants ( $K_D$ ) for EHF and ERG binding to different DNA sequences.**

ETS	DNA	$K_D$ (nM) <sup>1</sup>	n	$p^2$
EHF	SC1	$1.0 \pm 0.1$	6	-
EHF	SC1 C2A	$2.1 \pm 0.5$	6	$4 \times 10^{-6}$
EHF	<i>COPS8</i>	$2.4 \pm 1.4$	4	0.03
ERG	SC1	$0.7 \pm 0.2$	4	-
ERG	SC1 C2A	$11 \pm 5$	4	0.005
ERG	<i>COPS8</i>	$17 \pm 7$	5	0.002

<sup>1</sup>  $K_D$  values are listed as mean  $\pm$  standard deviation.

<sup>2</sup>  $p$ -values were calculated for EHF and ERG with comparison to SC1 DNA values.

**Table S3. Peak coordinates for ERG-FLAG and EHF-FLAG occupied regions in RWPE1 cells.**

See excel spreadsheet online for list of top 1000 ERG-FLAG and EHF-FLAG occupied regions in RWPE1 cells.

**Table S4. RSAT analysis of ETS-AP1 spacing in top 1000 peaks of ERG and EHF ChIP datasets.**

See excel spreadsheet online for list of RSAT matches from top 1000 ERG-FLAG and EHF-FLAG ChIP-Seq peaks to ETS-AP1 sites.

**Table S5. Equilibrium dissociation constants ( $K_D$ ) for EHF truncations binding to *COPS8* enhancer DNA with and without JUN-FOS.**

EHF	DNA	JUN-FOS <sup>1</sup>	$K_D$ (nM) <sup>2</sup>	n	$p$ <sup>3</sup>
EHF	<i>COPS8</i>	-	$3.7 \pm 0.5$	4	-
EHF <sup><math>\Delta</math>N183</sup>	<i>COPS8</i>	-	$3.3 \pm 0.5$	4	0.3
EHF <sup><math>\Delta</math>N193</sup>	<i>COPS8</i>	-	$3.2 \pm 0.7$	4	0.3
EHF <sup><math>\Delta</math>N203</sup>	<i>COPS8</i>	-	$3.5 \pm 0.6$	4	0.7
EHF	<i>COPS8</i>	+	$170 \pm 80$	4	-
EHF <sup><math>\Delta</math>N193</sup>	<i>COPS8</i>	+	$130 \pm 20$	4	0.4
EHF <sup><math>\Delta</math>N183</sup>	<i>COPS8</i>	+	$90 \pm 20$	4	0.1
EHF <sup><math>\Delta</math>N203</sup>	<i>COPS8</i>	+	$20 \pm 7$	4	0.01

<sup>1</sup> JUN <sup>$\Delta$ N250  $\Delta$ C319</sup>- FOS <sup>$\Delta$ N131  $\Delta$ C203</sup> proteins were used in this experiment.

<sup>2</sup>  $K_D$  values are listed as mean  $\pm$  standard deviation.

<sup>3</sup>  $p$ -values were calculated for EHF truncations with comparison to full-length EHF.

**Table S6. Equilibrium dissociation constants ( $K_D$ ) for EHF<sup>ΔN193</sup> mutants binding to *COPS8* enhancer DNA with and without JUN-FOS.**

EHF <sup>ΔN193</sup>	DNA	JUN-FOS <sup>1</sup>	$K_D$ (nM) <sup>2</sup>	n	$p^3$
WT	<i>COPS8</i>	-	5 ± 2	6	-
K196E/K200E/K201E	<i>COPS8</i>	-	5 ± 4	4	0.7
K241E/S242P/A244E	<i>COPS8</i>	-	4 ± 3	4	0.6
K251E/K252Q	<i>COPS8</i>	-	4 ± 2		0.5
K272E	<i>COPS8</i>	-	4 ± 3	4	0.9
WT	<i>COPS8</i>	+	120 ± 40	6	-
K196E/K200E/K201E	<i>COPS8</i>	+	5 ± 3	4	2 x 10 <sup>-4</sup>
K241E/S242P/A244E	<i>COPS8</i>	+	140 ± 30	4	0.4
K251E/K252Q	<i>COPS8</i>	+	50 ± 10	4	0.007
K272E	<i>COPS8</i>	+	20 ± 10	4	7 x 10 <sup>-4</sup>

<sup>1</sup> JUN<sup>ΔN250 ΔC319</sup>-FOS<sup>ΔN131 ΔC203</sup> proteins were used in this experiment.

<sup>2</sup>  $K_D$  values are listed as mean ± standard deviation.

<sup>3</sup>  $p$ -values were calculated for EHF truncations with comparison to full-length EHF.



**Table S7. Equilibrium dissociation constants ( $K_D$ ) for ETS truncations binding to *COPS8* enhancer DNA with and without JUN-FOS.**

ETS <sup>1</sup>	DNA <sup>1</sup>	JUN-FOS <sup>1</sup>	$K_D$ (nM) <sup>2</sup>	n
ERF <sup>ΔC126</sup>	<i>COPS8</i>	-	23 ± 2	2
ERF <sup>ΔC126</sup>	<i>COPS8</i>	+	6.5 ± 0.6	2
GABPA <sup>ΔN281</sup>	<i>COPS8</i>	-	3.7 ± 0.4	2
GABPA <sup>ΔN281</sup>	<i>COPS8</i>	+	3.5 ± 0.7	2
ELF1 <sup>ΔN148 ΔC313</sup>	<i>COPS8</i>	-	8 ± 3	2
ELF1 <sup>ΔN148 ΔC313</sup>	<i>COPS8</i>	+	50 ± 20	2
ELK4 <sup>ΔC330</sup>	<i>COPS8</i>	-	1.9 ± 0.5	2
ELK4 <sup>ΔC330</sup>	<i>COPS8</i>	+	1.0 ± 0.2	2

<sup>1</sup> JUN<sup>ΔN250 ΔC319</sup>- FOS<sup>ΔN131 ΔC203</sup> proteins were used in this experiment.

<sup>2</sup>  $K_D$  values are listed as mean ± standard deviation.

**Table S8. Protein and DNA sequences used in this study.**

Name <sup>1,2</sup>	Sequence <sup>3</sup>
JUN	MGSSHHHHHHSSGLVPRGSHMTAKMETTFYDDALNASFLPSESGPYGY SNPKILKQSM TLNLADPVGSLKPHLRKNSDLLTSPDVGLLKLASPELE RLIIQSSNGHITTTPTPTQFLCPKNVTDEQEGFAEGFVRALAE LHSQNTLP SVTSAAQPVNGAGMVAPAVASVAGGSGSGGFSASLHSEPPVYANLSNF NPGALSSGGGAPSYGAAGLAFPAQPQQQQPPHLLPQQMPVQHPR LQ ALKEEPQTVPEMPGETPPLSPIDMESQERIKAEKRMRNR IAASKCRKR KLERIARLEEKVKTLKAQNSELASTANMLREQVAQLKQKVMNHVNSG CQLMLTQQLQTF
JUN <sup>ΔN250 ΔC319</sup>	MGSSHHHHHHSSGLVPRGSHM QERIKAEKRMRNR IAASKCRKRKLER IARLEEKVKTLKAQNSELASTANMLREQVAQLKQKVMNHVNSG
FOS	MMFSGFNADYEASSSRCSSASPAGDSL SY YHSPADSFSSMGSPVNAQDF CTDLAVSSANFIPTVTAISTSPDLQWL VQPALVSSVAPSQTRAPHPFGVP APSAGAYS RAGVVK TMTGGRAQSIGRRGKVEQLSPEEEEEKRRIRRERN KMAAAKCRNRRREL TDTLQAETDQLEDEKSALQTEIANLLKEKEKLEFI LAAHRPACKIPDDLGFPEEMSVASLDLTGGLPEVATPESEEAF TLPLND PEPKPSVEPVKSISSMELKTEPFDDFLFPASSRPSGSETARV PDMDLSGS FYAADWEPLHSGSLGMGP MATELEPLCTPVVTCTP SCTAYTSSFVFTYP EADSFPSCAA AHRK GSSSNPSSDSLSSPTLLAL
FOS <sup>ΔN131 ΔC203</sup>	MGSSHHHHHHSSGLVPRGSHM QLSPEEEEEKRRIRRERNKMAAAKCRN RRREL TDTLQAETDQLEDEKSALQTEIANLLKEKEKLEFILAAHRPA
EHF	MGSSHHHHHHSSGLVPRGSHM IEGGGVMNLNPGNNLLHQPPAWTDS YSTCNVSSGFFGGQWHEIHPQY WTKYQVWEWLQHLLDTNQLDANCIP FQEFDINGEHLCSMSLQEFTRAAGTAGQLLYSNLQHLKWNGQCSSDLF QSTHNVIVKTEQTEPSIMNTWKDENYLYDTNYGSTVDLLDSKTF CRAQI SMTTTS HLPVAESPDMKKEQDPPAKCHTKKH NPRGTHL WEFIRDILLNP DKNPGLIKWEDRSEG VFRFLKSEAVAQLWGKKKNNSSMTYEKLSRAM RYYYKREILERVDGRRLVYKFGKNARGWRENEN
EHF <sup>ΔN183</sup>	MGSSHHHHHHSSGLVPRGSHM ESPDMKKEQDPPAKCHTKKH NPRGTH L WEFIRDILLNPDKNPGLIKWEDRSEG VFRFLKSEAVAQLWGKKKNNSS MTYEKLSRAMRYYYKREILERVDGRRLVYKFGKNARGWRENEN
EHF <sup>ΔN193</sup>	MGSSHHHHHHSSGLVPRGSHM PPAKCHTKKH NPRGTHL WEFIRDILLN PDKNPGLIKWEDRSEG VFRFLKSEAVAQLWGKKKNNSSMTYEKLSRA MRYYYKREILERVDGRRLVYKFGKNARGWRENEN
EHF <sup>ΔN193</sup> K196E/ K200E/ K201E	MGSSHHHHHHSSGLVPRGSHM PPAECHTEEHNPRGTHL WEFIRDILLN PDKNPGLIKWEDRSEG VFRFLKSEAVAQLWGKKKNNSSMTYEKLSRA MRYYYKREILERVDGRRLVYKFGKNARGWRENEN
EHF <sup>ΔN193</sup> K241E/ S242P/ A244E	MGSSHHHHHHSSGLVPRGSHM PPAKCHTKKH NPRGTHL WEFIRDILLN PDKNPGLIKWEDRSEG VFRFLPEEVAQLWGKKKNNSSMTYEKLSRA MRYYYKREILERVDGRRLVYKFGKNARGWRENEN

EHF<sup>ΔN193</sup>  
K251E/  
K252Q  
MGSSHHHHHHSSGLVPRGSHMPPAKCHTKKHNPGRGTHLWEFIRDILLN  
PDKNPGLIKWEDRSEGVFRFLKSEAVAQLWGGEQKNNSSMTYEKLSRA  
MRYYYKREILERVDGRRLVYKFGKNARGWRENEN

EHF<sup>ΔN193</sup>  
K272E  
MGSSHHHHHHSSGLVPRGSHMPPAKCHTKKHNPGRGTHLWEFIRDILLN  
PDKNPGLIKWEDRSEGVFRFLKSEAVAQLWGKKKNNSSMTYEKLSRA  
MRYYYEREILERVDGRRLVYKFGKNARGWRENEN

EHF<sup>ΔN203</sup>  
MGSSHHHHHHSSGLVPRGSHMNPRGTHLWEFIRDILLNPDKNPGLIKW  
EDRSEGVFRFLKSEAVAQLWGKKKNNSSMTYEKLSRAMRYYYKREIL  
ERVDGRRLVYKFGKNARGWRENEN

ELF1<sup>ΔN148 ΔC313</sup>  
MGSSHHHHHHSSGLVPRGSHMPEVMETQQVQEKYADSPGASSPEQPK  
RKKGRKTKPPRPDSPATTPNISVKKKNDGKGNITLWEFLALLQDK  
ATCPKYIKWTQREKGFKLVDSKAVSRLWGKHKNKPDMMNYETMGRAL  
RYYYQRGILAKVEGQRLVYQFKEMPKDLIYINDEDPSSSISSDP

ELK4<sup>ΔC330</sup>  
MGSSHHHHHHSSGLVPRGSHMDSAITLWQFLQLLQKPQNKHMICWT  
SNDGQFKLLQAEVARLWGIRKNKPNMNYDKLSRALRYYYVKNIIK  
VNGQKFVYKFVSYPEILNMDPMTVGRIEGDCESLNFSEVSSSSKDVENG  
GKDKPPQPGAKTSSRNDYIHSGLYSSFTLNSLNSSNVKLFKLIK TENPAE  
KLAEEKSPQEPTPSVIKFTTPSKKPPVEPVAATISIGPSISPSSEETIQALE  
TLVSPKLPSEAPTSASNVMATAFATTPPISSIPPLQEPPTSPPLSSHPDID  
TDIDSVASQPMELPENLSLEPKDQDSVLEKDKVNNSSRSKKPKGLELA  
PT

ERF<sup>ΔC126</sup>  
MGSSHHHHHHSSGLVPRGSHMKT PADTGFAFPDWAYKPESSPGSRQIQ  
LWHFILELLRKEEYQGVIAWQGDYGEFVIKDPDEVARLWGVRKCKPQ  
MNYDKLSRALRYYYNKRILHKTGKRFTYKFNFNKLVLVNYPFIDVGL  
AGG

ERG  
MGSSHHHHHHSSGLVPRGSHMASTIKEALS VVSEDQSLFECAYGTPHL  
AKTEMTASSSSDYGQTSKMSRPVQQDWLSQPPARVTIKMECNPSQVN  
GSRNSPDECSVAKGGKMVGSPDTVGMNYGSYMEEKHMPPPNMTTNE  
RRVIVPADPTLWSTDHVRQWLEWAVKEYGLPDVNILLFQNI DGKELCK  
MTKDDFQRLTPSYNADILLSHLHYLRETPLPHLTSDDVDKALQNSPRLM  
HARNTGGA FIFPNTSVYPEATQRITTRPDLPEPPRRAWTGHGHTP  
QSKAAQSPSTVPKTEDQRPQLDPYQILGPTSSRLANPGSGQIQLWQFL  
ELSDSSNSSCITWEGTNGEFKMTDPDEVARRWGERKSKPNMNYDKLS  
RALRYYYDKNIMTKVHGKRYAYKFDHFGIAQALQPHPESSLYKYPSD  
LPYMGSYHAHPQKMNFVAPHPPALPVTSSSFFAAPNPYWNSPTGGIYPN  
TRLPTSHMPSHLGTY

ETV1	MGSSHHHHHHSSGLVPRGSHMDGFYDQQVPYMTNSQRGRNCNEKPT NVRKRKFINRDLAHDSEELFQDLSQLQETWLAEAQVPDNDEQFVPDYQ AESLAFHGLPLKIKKEPHSPCSEISSACSQEOPFKFSYGEKCLYNVSAID QKPQVGMRPSNPPTSPSTPVSPLHHASPNSTHTPKPDRAFP AHLPPSQSIP DSSYPMDHRFRRLSEPCNSFPPLPTMPREGRPMYQRQMSEPNIPFPQ GFKQEYHDPVYEHNMTVGSAAASQSFPPPLMIKQEPRDFAYDSEVPSCHS IYMRQEGFLAHPSTRTEGCMFEKGPRQFYDDTCVVPEKFDGDIKQEPGM YREGPTYQRRGSLQLWQFLVALLDDPSNSHFIAWTGRGMEFKLIEPEEV ARRWGIQKNRPAMNYDKLSRSLRYYYEKGIMQKVAGERYVYKFCVDP EALFSMAFPDNQRPLLKTDMERHINEEDTVPLSHFDESMAYMPEGGCC NPHPYNEGYVY
ETV4	MGSSHHHHHHSSGLVPRGSHMERRMKAGYLDQQVPYTFSSKSPGNGS LREALIGPLGKLMDPGSLPPLDSEDLFQDLSHFQETWLAEAQVPDSDEQ FVPDFHSENLAHSPTRIKKEPQSPRTDPALSCSRKPPLPYHHGEQCLY SSAYDPPRQIAIKSPAPGALGQSPLQPFPRAEQRNFLRSSGTSQPHPGHG YLGEHSSVFQQPLDICHSTFSQGGGREPLPAPYQHQLSEPCPPYPQQSFK QEYHDPLYEQAGQPAVDQGGVNGHRYPGAGVVIKQEQTDFAYDSVDT GCASMYLHTEGFSGPSGDGAMGYGYEKPLRPFDDVCVVPEKFEGDI KQEGVGAFFREGPPYQRRGALQLWQFLVALLDDPTNAHFIAWTGRGME FKLIEPEEVARLWGIQKNRPAMNYDKLSRSLRYYYEKGIMQKVAGERY VYKFCVCEPEALFSLAFP DNQRPALKA EFD RPVSEEDTVPLSHLDESPAY LPELAGPAQPFPGKGGYSY
FLI1	MGSSHHHHHHSSGLVPRGSHMDGTIKEALS VVSDDQSLFDSAYGAAA HLPKADMTASGSPDYGQPHKINLPPQQEWINQPV RVNVKREYDHMN GSRESPVDCSVSKCNKLVGGGEANPMNYSYMDKNGPPPPNMTNE RRVIVPADPTLWTQEHVRQWLEWAIKEYGLMEIDTSFFQNMDGKELCK MNKEDFLRATSAYNTEVLLSHLSYLRESSLLAYNTTSHTDQSSRLNVKE DPSYDSVRRGAWNNMNSGLNKSPLLGGSQTMGKNTEQRQPDPYQI LGPTSSRLANPGSGQIQLWQFLLELLSDSANASCITWEGTNGEFKMTDP DEVARRWGERKSKPNMNYDKLSRALRYYYDKNIMTKVHGKRYAYKF DFHGIAQALQPHPTETSMYKYPSDISYMP SYHAHQKVN FVSPHPSSMP VTSSSFFGAASQYWTSP TAGIYPNPSVPRHPNTHVPSHLGSYY
GABPA <sup>ΔN281</sup>	MGSSHHHHHHSSGLVPRGSHMPTTIKVINSSAKAAKVQRAPRISGEDRS SPGNRTGNNGQIQLWQFLLELLTDKDARD CISWVGDEGEFKNQPELV AQKWGQRKNKPTMNYEKLSRALRYYYDGMICKVQGRFVYKFCVCD LKTLLIGYSA AELNRLVTECEQKKLAKMQLHGIAQPVT AVALATASLQT EKDN
<i>UPP</i>	<u>TAGGGGAAATGACTCATTCA</u>
<i>COPS8</i>	<u>TCGAAGAGAGGAAGTGACTCAGCCC</u>
SC1	<u>TCGACGGCCAAGCCGGAAGTGAGTGCC</u>
SC1 C2A	<u>TCGACGGCCAAGCAGGAAGTGAGTGCC</u>

<sup>1</sup>Residues included in truncated proteins are indicated by superscript; proteins without superscript are full length.

<sup>2</sup>Gene promoter or enhancer DNA sequences are denoted in italic. SC1 refers to “selected clone 1”, a consensus high-affinity ETS binding sequence (1).

<sup>3</sup>ETS and AP1 DNA binding sites are underlined, mutations to protein and DNA sequences are emboldened.

**Table S9. qPCR primer sequences used in this study.**

Genomic coordinates	Gene	Fwd/Rev	Primer Sequence
chr8:131918646-131919405	ADCY8	Fwd	ATGCTGAAACTGGCCCAGAA
chr8:131918646-131919405	ADCY8	Rev	TCCAGGGTGGTAGAGAGACG
chr5:94417054-94417894	MCTP1	Fwd	CGGCAAAGAGGCTGTTCAC
chr5:94417054-94417894	MCTP1	Rev	TCATTCCAAGTCGCTGCTGT
chr19:11205375-11206235	LDLR	Fwd	CCCTCGTACAGAGGTAGGGA
chr19:11205375-11206235	LDLR	Rev	ATCACCCCACTAGGTGACCG
chr6:136931277-136931996	MAP3K5	Fwd	CTCAGTGGTTGCGTTGCCTA
chr6:136931277-136931996	MAP3K5	Rev	GGTTGACTCCCCTACTCCAC
chr9:73053231-73053934	KLF9	Fwd	GCTGGGAAGGAAGGTTCTGG
chr9:73053231-73053934	KLF9	Rev	AAAGACCCACATGGCTTGCT
chr20:7837265-7837937	PLCB1	Fwd	ATGGCTGTCTAACTTTGCCCC
chr20:7837265-7837937	PLCB1	Rev	AGTTCAAGACGATTGCCAGGT
chr12:31901844-31902653	AMN1	Fwd	TGTGGATTGGTTGGGGGATG
chr12:31901844-31902653	AMN1	Rev	ACCGTGA CTGCAACAAAGGA
chr12:109231955-109232747	SSH1	Fwd	GAGGGCCTCTCACATACACG
chr12:109231955-109232747	SSH1	Rev	GTGGTCTCCGAGCAGGAAAA
chr6:148762145-148763173	SASH1	Fwd	GAGTGAACGGGCTGTAGCTT
chr6:148762145-148763173	SASH1	Rev	TTCTGAGGGAACACCTGAGC
chr16:55786521-55787940	CES1P2	Fwd	TGGGGTGGGAAAGTTGTAGC
chr16:55786521-55787940	CES1P2	Rev	TGGACTGTACCTTCCCCGAT
chr13:114102955-114104117	ADPRHL1	Fwd	TGTGCTCACTCTAGCAGCAG
chr13:114102955-114104117	ADPRHL1	Rev	AAAGTCCTTACCCCCACGAG
chr17:41465400-41467142	LINC00910	Fwd	AGAGACCTGTAGGCGGAGAG
chr17:41465400-41467142	LINC00910	Rev	CCCACTGGTGACGACGTAAA
chr1:1724266-1724486	CDK11A	Fwd	CGCAGTTTCTTTTGGAGTCCTG
chr1:1724266-1724486	CDK11A	Rev	TCGGA ACTCACCCCTACGGG
chr7:6424763-6425534	RAC1	Fwd	GGGCCTGTAATCTGCCTTG
chr7:6424763-6425534	RAC1	Rev	GAGCCCTTCTCTCTGCTGTG
chr7:31532974-31534069	CCDC129	Fwd	TCTGAAAGTGGGGACTTGGC
chr7:31532974-31534069	CCDC129	Rev	ACTCATCTGGGAGTCTGGGG
chr16:15684488-15685337	MARF1	Fwd	GCCTCTGGTACTTCCGCTAAG
chr16:15684488-15685337	MARF1	Rev	GAAGGTGGCCCTGGTAATCT
chr5:134475533-134477670	c5orf66	Fwd	AGGCAGGGACTAGCTCTGAA
chr5:134475533-134477670	c5orf66	Rev	CGAGGCTGATGCTCAGAGAG
chr20:45988666-45989914	ZMYND8	Fwd	CTGCATCCCGAGATAGCCTG
chr20:45988666-45989914	ZMYND8	Rev	TCCATTTCCGCTAACGGTCA

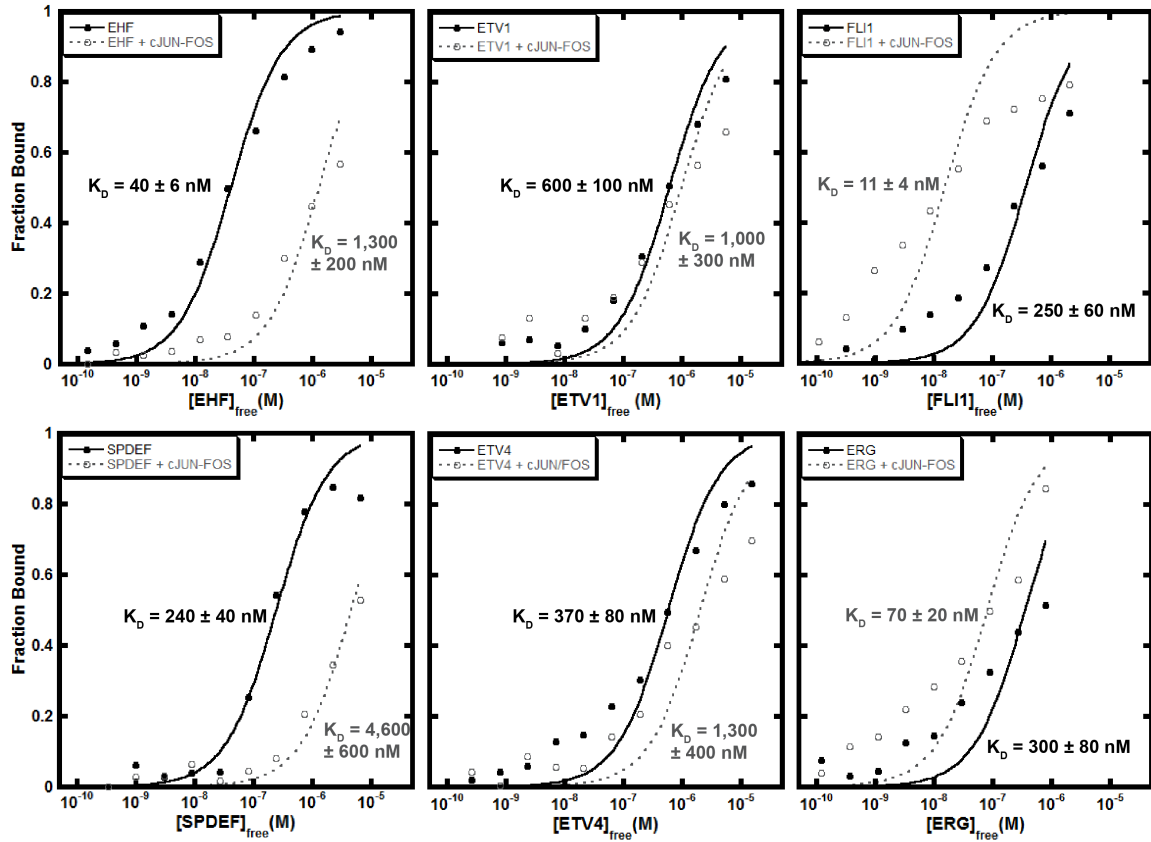


**Figure S1. JUN-FOS differentially influences the DNA binding of ETS factors.** Binding isotherms for ETS factors binding to *UPP* promoter DNA in the absence (black) or presence of JUN-FOS (gray). Each data point is the mean from two replicates. See Methods for details.

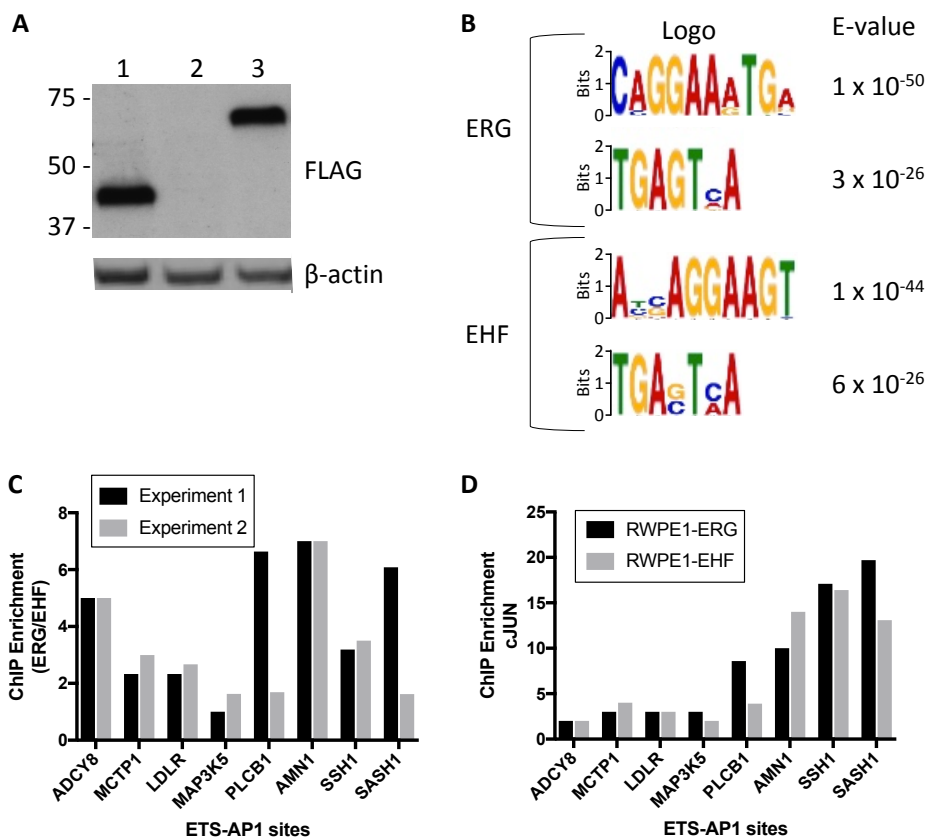


**Figure S2.** ETS and AP1 sites are overrepresented at ERG- and EHF- bound genomic regions. *A*, Western blot of lysates from cells infected with EHF-FLAG (lane 1), empty control (lane 2), and ERG-FLAG (lane 3) retroviruses. FLAG-tagged ERG and EHF were expressed at similar levels upon retroviral expression in RWPE1 cells. *B*, Full AP1 DNA-binding sequences (TGANTCA) were overrepresented in both ERG-FLAG and EHF-FLAG ChIP datasets, as determined by MEME (2). Note that despite the overrepresentation of AP1 DNA-binding sequences in both datasets, the closely spaced ETS-AP1 composite sites were more frequently observed for ERG than for EHF (Fig. 3B). *C*, Ratio of ERG and EHF enrichment at the eight ETS-AP1 sites in Figure 3C. Replicate qPCRs from two experiments are shown for each region. *D*, Comparison of JUN enrichment at ETS-AP1 sites in RWPE1 cells expressing ERG-FLAG (black) and EHF-FLAG (gray). JUN enrichment was similar at most sites but depleted at PLCB1 and SASH1 ETS-AP1 sites in RWPE1 cells expressing EHF-FLAG. Two to three independent biological replicates provided similar patterns, but different maximum levels of enrichment. A representative experiment is shown.

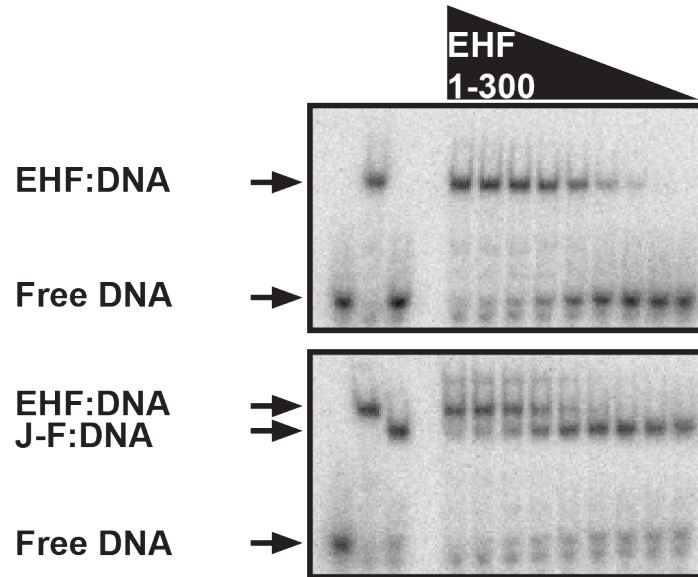


**Figure S3.** The minimal DNA-binding domains of JUN and FOS are sufficient for anticooperative DNA binding with EHF. *COPS8* enhancer DNA was titrated with EHF by itself (top) and with near saturating amounts of JUN-FOS DNA-binding domains (JUN<sup>ΔN250 ΔC319</sup> and FOS<sup>ΔN131 ΔC203</sup>) (bottom). Similar levels of anticooperative binding that were observed with JUN-FOS DNA-binding domains as with full-length JUN-FOS (Fig. 1). Therefore, JUN-FOS DNA-binding domains are sufficient for anticooperative DNA binding with EHF.



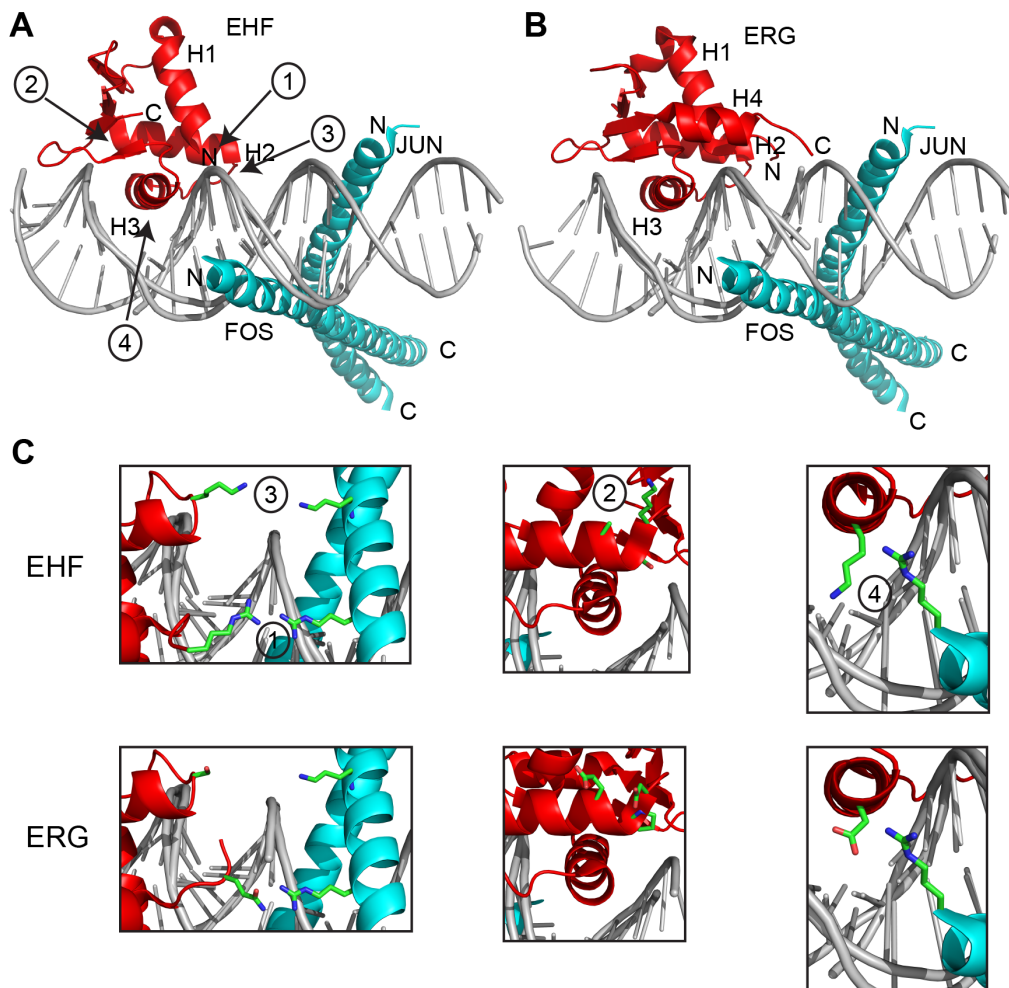


**Figure S4. EHF and ERG have distinct JUN-FOS interfaces.** Model of EHF, *A*, and ERG, *B*, binding to an ETS-AP1 composite DNA sequence with JUN-FOS. Models are oriented as in Fig. 5A,B, and proteins are shown in cartoon format. *C*, Model of EHF (top) and ERG (bottom) zoomed in on regions of EHF that were mutated in Fig. 5C-D. Positively charged residues in EHF along the JUN-FOS interface are shown in stick format, as well as the corresponding residues in ERG.



**Figure S5. Alignment of ETS domain and flanking sequences for human ETS factors.** Sequences corresponding to the ETS domain and flanking regions (up to 60 residues on each side or until the native amino- and carboxy-terminus) were aligned using Clustal Omega (3). The secondary structure of the conserved ETS domain is illustrated above the sequences;  $\alpha$ -helices are represented as cylinders and  $\beta$ -strands are represented as arrows. Black arrows underneath the sequences refer to amino acids that were mutated in EHF that contribute to anticeoperative DNA binding with JUN-FOS (Fig. 5C). High density of positive residues at the amino terminus of the SPI, ELF1/2/4, and EHF subfamilies are boxed in blue. SPI1 was previously observed to bind to DNA in an anticeoperative fashion with JUN-FOS (4), and we show that EHF and ELF1 behave similarly in this manuscript. Therefore, we suggest that ETS factors that bind to DNA anticeoperatively with JUN-FOS possess a positive interface composed of residues from the amino terminal region of the ETS domain, the loop between  $\alpha$ -helices H2 and H3, and the carboxy-terminus of  $\alpha$ -helix H3.

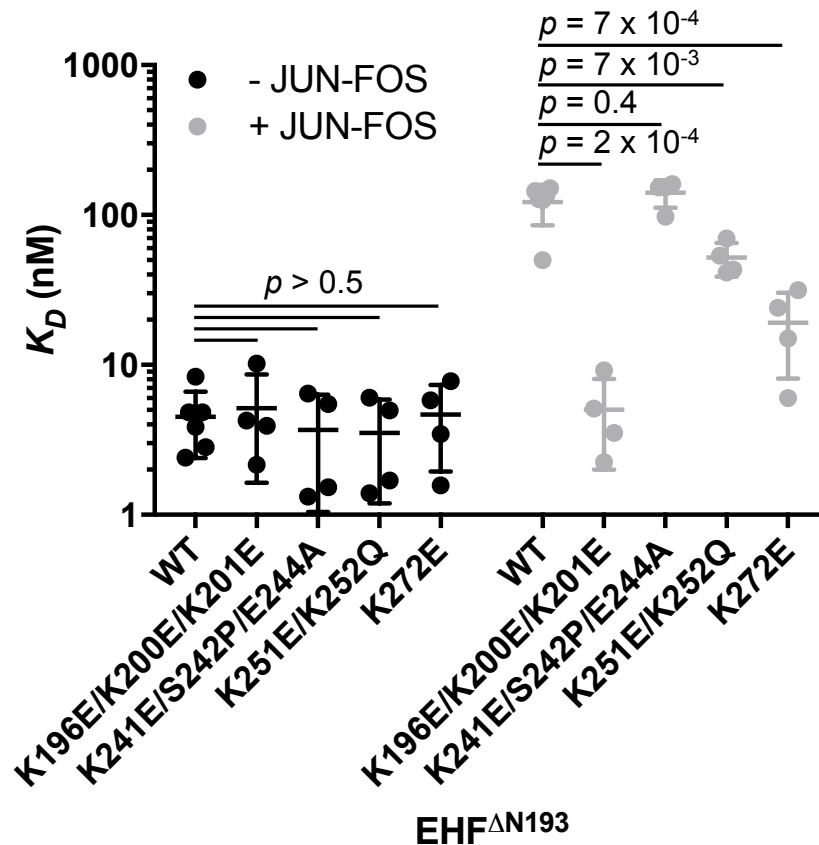


**Figure S6. Positive residues on the JUN-FOS interface of EHF mediate anticooperative DNA binding.** EMSAs were performed for EHF $\Delta$ N193 wildtype (WT) and indicated mutants alone (black), and with near-saturating amounts of JUN $\Delta$ N250  $\Delta$ C319-FOS $\Delta$ N131  $\Delta$ C203 (gray). Each closed circle represents the  $K_D$  for EHF from a single experiment; at least four replicate experiments were performed with each EHF protein. Bars represent the mean and standard deviation for each dataset, and  $p$  values comparing EHF proteins are displayed. Mean, standard deviation, number of replicates, and  $p$  values are listed in Table S6. Representative EMSAs for each version of EHF with JUN $\Delta$ N250  $\Delta$ C319-FOS $\Delta$ N131  $\Delta$ C203 are shown in Figure 5D. The mutation of positive residues on the JUN-FOS interface (K196E/K200E/K201E, K251E/K252Q, and K272E; see Figure 5A and Figure S4 for residue locations) enhances EHF binding to DNA with JUN-FOS, but does not alter EHF binding to DNA alone.

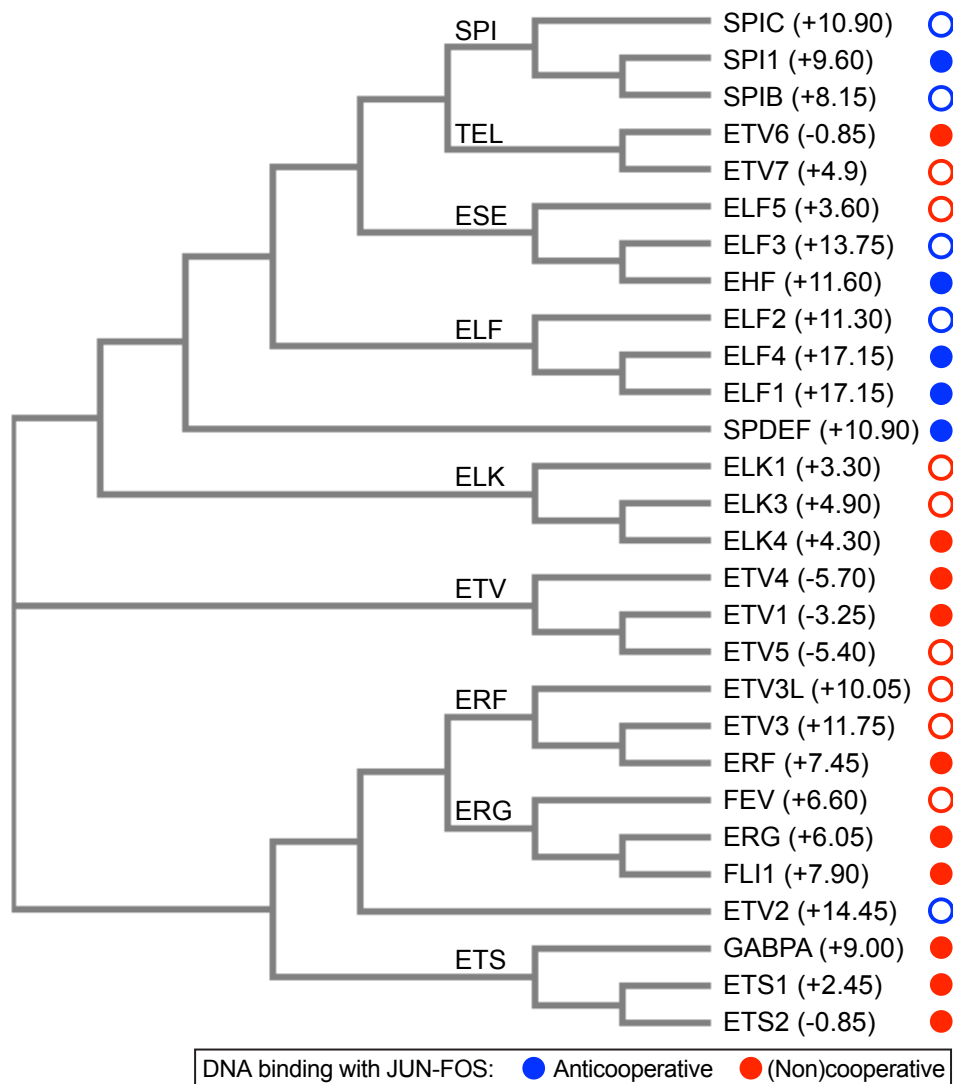


**Figure S7. Diversification of charge in ETS factor evolution.** A dendrogram of ETS domain and flanking sequences (up to sixty residues on each side of the ETS domain) shows the degree of relatedness for 28 human ETS factors. Subfamilies are named on the left, following previous nomenclature (5), and individual ETS factors are named on the right. The number indicates the net charge of the ETS domain and flanking sequences. Circles indicate DNA binding of each ETS factor with JUN-FOS. Blue circles indicate anticooperative binding with JUN-FOS, and red circles indicate noncooperative or cooperative binding with JUN-FOS. Closed circles are based on experimental evidence in this study or previously (4). Open circles are predictions based on sequence alignment (Fig. S5). The dendrogram illustrates a large extent of clustering between ETS factors that bind to DNA anticooperatively with JUN-FOS at the top, and those that bind to DNA noncooperatively or cooperatively at the bottom.

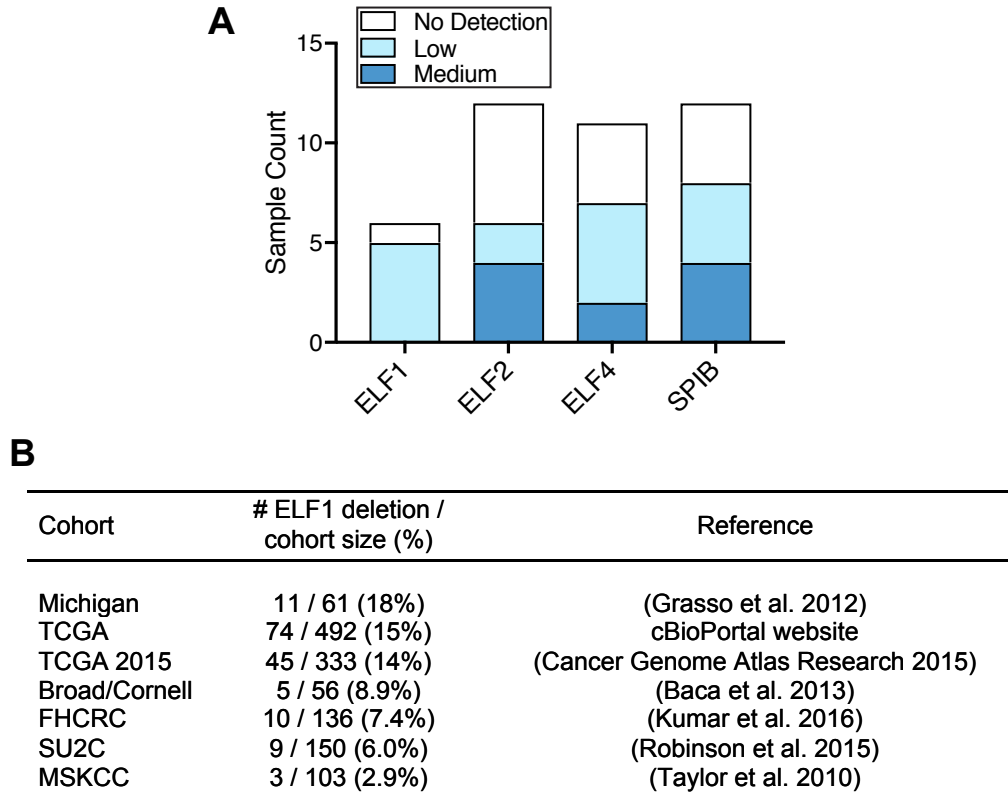


**Figure S8. The ELF1 gene is frequently deleted in prostate cancer patients.** *A*, Count of prostate cancer samples displaying relative protein levels of ELF1, ELF2, ELF4, and SPIB from the Protein Atlas (6,7). All of these proteins are present at a “medium” level in normal prostate samples; therefore, “low” or “no detection” represents a reduction in protein levels in cancer samples. *B*, Compilation of prostate cancer studies that found deletion of the ELF1 gene in greater than one percent of tested patients. Data was compiled from cBioPortal (8,9) using previously published prostate cancer studies (10-15).

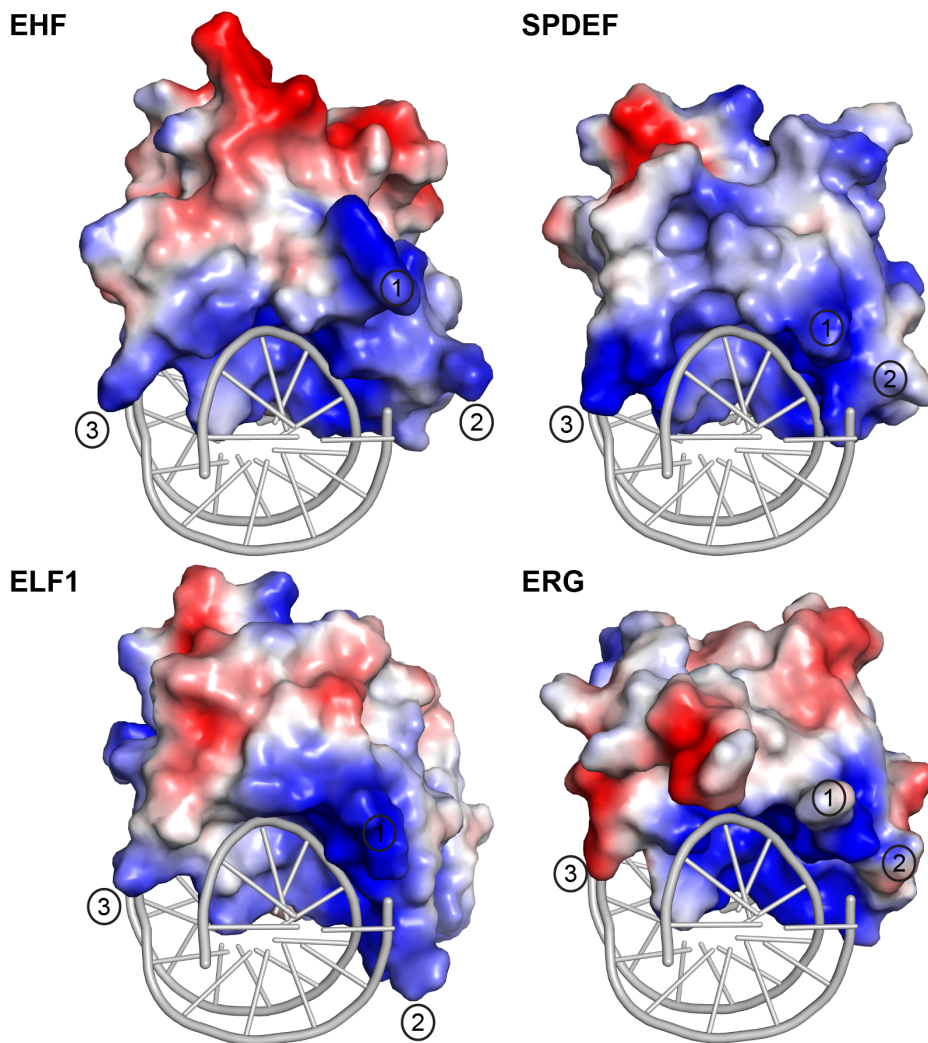


**Figure S9. Positively charged JUN-FOS interface on tumor suppressor ETS factors prevents simultaneous DNA binding at composite ETS-AP1 sites.** Structures of EHF (homology model based on PDB entry 3JTG), SPDEF (1YO5), ELF1 (homology model based on 3JTG), and ERG (4IRI) bound to DNA. Images are oriented from the perspective of JUN-FOS, so the proximal region near DNA is the contact surface for JUN-FOS. Regions that are mutated in EHF in Figure 5 are notated; (1) N-terminal of ETS domain, (2) H2-H3 loop, (3) C-terminus of H3. The positively charged residues in all of these regions for EHF, SPDEF, and ELF1 are necessary for anticooperative DNA binding with JUN-FOS. In contrast, the relative lack of positive charges in these regions allows ERG to simultaneously bind to DNA with JUN-FOS. Note that all ETS factors possess a conserved basic DNA-binding interface. Thus, a basic interface that is variably present in ETS factors is able to selectively control transcription factor partnerships.

## Supplementary References

1. Nye, J. A., Petersen, J. M., Gunther, C. V., Jonsen, M. D., and Graves, B. J. (1992) Interaction of murine ets-1 with GGA-binding sites establishes the ETS domain as a new DNA-binding motif. *Genes Dev* **6**, 975-990
2. Machanick, P., and Bailey, T. L. (2011) MEME-ChIP: motif analysis of large DNA datasets. *Bioinformatics* **27**, 1696-1697
3. Sievers, F., Wilm, A., Dineen, D., Gibson, T. J., Karplus, K., Li, W., Lopez, R., McWilliam, H., Remmert, M., Soding, J., Thompson, J. D., and Higgins, D. G. (2011) Fast, scalable generation of high-quality protein multiple sequence alignments using Clustal Omega. *Mol Syst Biol* **7**, 539
4. Kim, S., Denny, C. T., and Wisdom, R. (2006) Cooperative DNA binding with AP-1 proteins is required for transformation by EWS-Ets fusion proteins. *Mol Cell Biol* **26**, 2467-2478
5. Hollenhorst, P. C., McIntosh, L. P., and Graves, B. J. (2011) Genomic and biochemical insights into the specificity of ETS transcription factors. *Annu Rev Biochem* **80**, 437-471
6. Uhlen, M., Fagerberg, L., Hallstrom, B. M., Lindskog, C., Oksvold, P., Mardinoglu, A., Sivertsson, A., Kampf, C., Sjostedt, E., Asplund, A., Olsson, I., Edlund, K., Lundberg, E., Navani, S., Szgyarto, C. A., Odeberg, J., Djureinovic, D., Takanen, J. O., Hober, S., Alm, T., Edqvist, P. H., Berling, H., Tegel, H., Mulder, J., Rockberg, J., Nilsson, P., Schwenk, J. M., Hamsten, M., von Feilitzen, K., Forsberg, M., Persson, L., Johansson, F., Zwahlen, M., von Heijne, G., Nielsen, J., and Ponten, F. (2015) Proteomics. Tissue-based map of the human proteome. *Science* **347**, 1260419
7. Uhlen, M., Zhang, C., Lee, S., Sjostedt, E., Fagerberg, L., Bidkhor, G., Benfeitas, R., Arif, M., Liu, Z., Edfors, F., Sanli, K., von Feilitzen, K., Oksvold, P., Lundberg, E., Hober, S., Nilsson, P., Mattsson, J., Schwenk, J. M., Brunnstrom, H., Glimelius, B., Sjoblom, T., Edqvist, P. H., Djureinovic, D., Micke, P., Lindskog, C., Mardinoglu, A., and Ponten, F. (2017) A pathology atlas of the human cancer transcriptome. *Science* **357**
8. Cerami, E., Gao, J., Dogrusoz, U., Gross, B. E., Sumer, S. O., Aksoy, B. A., Jacobsen, A., Byrne, C. J., Heuer, M. L., Larsson, E., Antipin, Y., Reva, B., Goldberg, A. P., Sander, C., and Schultz, N. (2012) The cBio cancer genomics portal: an open platform for exploring multidimensional cancer genomics data. *Cancer Discov* **2**, 401-404
9. Gao, J., Aksoy, B. A., Dogrusoz, U., Dresdner, G., Gross, B., Sumer, S. O., Sun, Y., Jacobsen, A., Sinha, R., Larsson, E., Cerami, E., Sander, C., and Schultz, N. (2013) Integrative analysis of complex cancer genomics and clinical profiles using the cBioPortal. *Sci Signal* **6**, p11
10. Grasso, C. S., Wu, Y. M., Robinson, D. R., Cao, X., Dhanasekaran, S. M., Khan, A. P., Quist, M. J., Jing, X., Lonigro, R. J., Brenner, J. C., Asangani, I. A., Ateeq, B., Chun, S. Y., Siddiqui, J., Sam, L., Anstett, M., Mehra, R., Prensner, J. R., Palanisamy, N., Ryslik, G. A., Vandin, F., Raphael, B. J., Kunju, L. P., Rhodes, D. R., Pienta, K. J., Chinnaiyan, A. M., and Tomlins, S. A. (2012) The mutational landscape of lethal castration-resistant prostate cancer. *Nature* **487**, 239-243
11. Cancer Genome Atlas Research, N. (2015) The Molecular Taxonomy of Primary Prostate Cancer. *Cell* **163**, 1011-1025
12. Baca, S. C., Prandi, D., Lawrence, M. S., Mosquera, J. M., Romanel, A., Drier, Y., Park, K., Kitabayashi, N., MacDonald, T. Y., Ghandi, M., Van Allen, E., Kryukov, G. V., Sboner, A., Theurillat, J. P., Soong, T. D., Nickerson, E., Auclair, D., Tewari, A., Beltran, H., Onofrio, R. C., Boysen, G., Guiducci, C., Barbieri, C. E., Cibulskis, K., Sivachenko, A., Carter, S. L., Saksena, G., Voet, D., Ramos, A. H., Winckler, W., Cipicchio, M., Ardlie, K., Kantoff, P. W., Berger, M. F., Gabriel, S. B., Golub, T. R.,

- Meyerson, M., Lander, E. S., Elemento, O., Getz, G., Demichelis, F., Rubin, M. A., and Garraway, L. A. (2013) Punctuated evolution of prostate cancer genomes. *Cell* **153**, 666-677
13. Kumar, A., Coleman, I., Morrissey, C., Zhang, X., True, L. D., Gulati, R., Etzioni, R., Bolouri, H., Montgomery, B., White, T., Lucas, J. M., Brown, L. G., Dumpit, R. F., DeSarkar, N., Higano, C., Yu, E. Y., Coleman, R., Schultz, N., Fang, M., Lange, P. H., Shendure, J., Vessella, R. L., and Nelson, P. S. (2016) Substantial interindividual and limited intraindividual genomic diversity among tumors from men with metastatic prostate cancer. *Nat Med* **22**, 369-378
  14. Robinson, D., Van Allen, E. M., Wu, Y. M., Schultz, N., Lonigro, R. J., Mosquera, J. M., Montgomery, B., Taplin, M. E., Pritchard, C. C., Attard, G., Beltran, H., Abida, W., Bradley, R. K., Vinson, J., Cao, X., Vats, P., Kunju, L. P., Hussain, M., Feng, F. Y., Tomlins, S. A., Cooney, K. A., Smith, D. C., Brennan, C., Siddiqui, J., Mehra, R., Chen, Y., Rathkopf, D. E., Morris, M. J., Solomon, S. B., Durack, J. C., Reuter, V. E., Gopalan, A., Gao, J., Loda, M., Lis, R. T., Bowden, M., Balk, S. P., Gaviola, G., Sougnez, C., Gupta, M., Yu, E. Y., Mostaghel, E. A., Cheng, H. H., Mulcahy, H., True, L. D., Plymate, S. R., Dvinge, H., Ferraldeschi, R., Flohr, P., Miranda, S., Zafeiriou, Z., Tunariu, N., Mateo, J., Perez-Lopez, R., Demichelis, F., Robinson, B. D., Sboner, A., Schiffman, M., Nanus, D. M., Tagawa, S. T., Sigaras, A., Eng, K. W., Elemento, O., Sboner, A., Heath, E. I., Scher, H. I., Pienta, K. J., Kantoff, P., de Bono, J. S., Rubin, M. A., Nelson, P. S., Garraway, L. A., Sawyers, C. L., and Chinnaiyan, A. M. (2015) Integrative Clinical Genomics of Advanced Prostate Cancer. *Cell* **162**, 454
  15. Taylor, B. S., Schultz, N., Hieronymus, H., Gopalan, A., Xiao, Y., Carver, B. S., Arora, V. K., Kaushik, P., Cerami, E., Reva, B., Antipin, Y., Mitsiades, N., Landers, T., Dolgalev, I., Major, J. E., Wilson, M., Socci, N. D., Lash, A. E., Heguy, A., Eastham, J. A., Scher, H. I., Reuter, V. E., Scardino, P. T., Sander, C., Sawyers, C. L., and Gerald, W. L. (2010) Integrative genomic profiling of human prostate cancer. *Cancer Cell* **18**, 11-22